

Article

An Algerian Soil-Living *Streptomyces alboflavus* Strain as Source of Antifungal Compounds for the Management of the Pea Pathogen *Fusarium oxysporum* f. sp. *pisi*

Marco Masi ^{1,*}, Dorsaf Nedjar ^{2,†}, Moustafa Bani ^{2,*}, Ivana Staiano ³, Maria Michela Salvatore ¹, Karima Khenaka ², Stefany Castaldi ³, Jesus Garcia Zorrilla ^{1,4}, Anna Andolfi ¹, Rachele Isticato ³ and Alessio Cimmino ¹

¹ Department of Chemical Sciences, University of Naples Federico II, Complesso Universitario Monte S. Angelo, Via Cinthia 4, 80126 Naples, Italy; mariamichela.salvatore@unina.it (M.M.S.); jesus.zorrilla@uca.es (J.G.Z.); andolfi@unina.it (A.A.); alessio.cimmino@unina.it (A.C.)

² Laboratory of Biotechnology, Higher National School of Biotechnology Taoufik Khaznadar, Nouveau Pôle Universitaire Ali Mendjeli, BP. E66, Constantine 25100, Algeria; dorsafnedjar0@gmail.com (D.N.); khenakak@yahoo.fr (K.K.)

³ Department of Biology, University of Naples Federico II, Complesso Universitario Monte S. Angelo, Via Cinthia 4, 80126 Naples, Italy; ivana.staiano@unina.it (I.S.); stefany.castaldi@unina.it (S.C.); isticato@unina.it (R.I.)

⁴ Allelopathy Group, Department of Organic Chemistry, Facultad de Ciencias, Institute of Biomolecules (INBIO), University of Cadiz, C/Avenida República Saharaui, s/n, 11510 Puerto Real, Spain

* Correspondence: marco.masi@unina.it (M.M.); m.bani@ensbiotech.edu.dz (M.B.)

† These authors contributed equally to this work.

Abstract: *Fusarium* wilt caused by *Fusarium oxysporum* f. sp. *pisi* (*Fop*) poses significant threats to pea cultivation worldwide. Controlling this disease is mainly achieved through the integration of various disease management procedures, among which biological control has proven to be a safe and effective approach. This study aims to extract and identify antifungal secondary metabolites from *Streptomyces alboflavus* KRO3 strain and assess their effectiveness in inhibiting the in vitro growth of *Fop*. This bacterial strain exerts in vitro antagonistic activity against *Fop*, achieving highly significant inhibition over one week. The ethyl acetate extract, obtained from its ISP2 agar medium culture, also exhibited strong antifungal activity, maintaining an inhibition rate of approximately 90% at concentrations up to 250 µg/plug compared to the control. Thus, the organic extract has been fractionated using chromatographic techniques and its bioguided purification allowed us to isolate the main bioactive compound. This latter was identified as metacycloprodigiosin using nuclear magnetic resonance (NMR) spectroscopy, electrospray ionization mass spectrometry (ESI-MS), and specific optical rotation data. Metacycloprodigiosin demonstrates dose-dependent inhibitory activity against the phytopathogen with an effective concentration of 125 µg/plug. The other secondary metabolites present in the ethyl acetate extract were also identified by gas chromatography–mass spectrometry (GC-MS) and nuclear magnetic resonance (NMR). This study highlighted the potential of *S. alboflavus* KRO3 strain and its antimicrobial compounds for the management of the pea pathogen *Fusarium oxysporum* f. sp. *pisi*.

Keywords: fusarium wilt; *Fusarium oxysporum*; *Streptomyces* sp.; antimicrobial compounds; prodiginine natural products; metacycloprodigiosin



Citation: Masi, M.; Nedjar, D.; Bani, M.; Staiano, I.; Salvatore, M.M.; Khenaka, K.; Castaldi, S.; Zorrilla, J.G.; Andolfi, A.; Isticato, R.; et al. An Algerian Soil-Living *Streptomyces alboflavus* Strain as Source of Antifungal Compounds for the Management of the Pea Pathogen *Fusarium oxysporum* f. sp. *pisi*. *J. Fungi* **2024**, *10*, 783. <https://doi.org/10.3390/jof10110783>

Academic Editor: Zonghua Wang

Received: 26 October 2024

Revised: 7 November 2024

Accepted: 8 November 2024

Published: 12 November 2024



Copyright: © 2024 by the authors. Licensee MDPI, Basel, Switzerland. This article is an open access article distributed under the terms and conditions of the Creative Commons Attribution (CC BY) license (<https://creativecommons.org/licenses/by/4.0/>).

1. Introduction

Fusarium wilt caused by *Fusarium oxysporum* f. sp. *pisi* (*Fop*) is an important damaging disease of field pea crops, as it has the potential to cause devastating yield losses of up to 100% in optimal conditions [1–3]. Its control is mainly achieved through the integration of various disease management procedures including chemical fungicides [4], resistant

cultivars and breeding [5], as well as agronomic and farming practices [6,7]. However, wilt remains a major problem due to the highly variable nature of the pathogen, in addition to the adverse environmental and health consequences of used chemicals. Thus, biological management using microbial biocontrol agents may provide a sustainable, cost-effective, and environmentally friendly alternative approach to prevent fusarium wilt [2,8]. In this respect, Actinobacteria have garnered significant attention for their antifungal properties against plant pathogenic fungi [9]. These Gram-positive bacteria possess substantial biosynthetic capacity to produce a wide array of structurally diverse secondary metabolites with remarkable biological activities [10]. Notably, research indicates that approximately 70% of known antimicrobial and antifungal compounds are derived from Actinobacteria [11–13]. These extensive biosynthetic capabilities position them as valuable sources for the discovery and development of novel antifungal compounds for the management of plant disease, particularly fusarium wilt. Among the Actinobacteria, *Streptomyces* species are of exceptional interest as they are a potential source of antimicrobial compounds that play a crucial role in protecting plants against phytopathogen attacks [13–15]. In this context, the present work focuses on the chemical and biological characterization of the major bioactive metabolite produced by an Algerian soil-living *Streptomyces alboflavus* presenting significant, *in vitro*, antifungal activity against *F. oxysporum* f. sp. *pisi*.

2. Materials and Methods

2.1. General Experimental Procedures

Analytical and preparative thin-layer chromatography (TLC) was performed on silica gel (Kieselgel 60, F₂₅₄, 0.25 and 0.5 mm, respectively; Merck, Darmstadt, Germany). Spots were visualized by exposure to UV radiation (254 nm) and by spraying with 10% H₂SO₄ in methanol (MeOH) (*v/v*), followed by heating at 110 °C for 10 min. Sigma-Aldrich Co. (St. Louis, MO, USA) supplied all the solvents. ¹H and ¹³C NMR spectra were recorded in deuterated chloroform (CDCl₃) at 400/100 MHz on Bruker (Karlsruhe, Germany) Anova Advance spectrometer and the same solvent was used as internal standard. Optical rotations were measured on a Jasco P-1010 digital polarimeter (Tokyo, Japan). HRESI-TOF mass spectra were measured on an Agilent Technologies ESI-TOF 6230DA instrument in the positive ion mode (Milan, Italy).

2.2. Microorganism and Culture Conditions

The bacterial isolate KRO3, exhibiting broad-spectrum antifungal activity against *Fusarium oxysporum*, was isolated from the rhizosphere of *Capsicum annuum* cultivated in the locality of Guelma (36°29' N, 07°30' E) in Northeastern Algeria. The dry soil sample was subjected to serial dilutions and bacterial isolation was conducted as previously described [16]. The purified strain was inoculated on ISP2 agar (Yeast extract 4 g/L, Malt extract 10 g/L, Dextrose 4 g/L, Agar 20 g/L and pH 7.2) The pure culture with 20% (*v/v*) glycerol was prepared and stored at –20 °C as spores and mycelial fragments.

After genomic DNA extraction performed as previously described [17,18], the 16S rDNA was amplified using the universal primers F27 (5'AGAGTTTGATCCTGGCTCAG3') and R1492 (5'TACGGCTACCTTGTACGACTT3') [19]. Consensus sequences were analysed using both BLAST (<http://www.ncbi.nlm.nih.gov/BLAST>, accessed on 15 September 2024) and EzTaxon server [20]. The bacterial isolate was identified as a member of the *Streptomyces* genus and exhibited 99.57% similarity with *Streptomyces alboflavus* NRRL B-2373^T. The sequence was deposited in GenBank under accession number PQ328212.

2.3. In Vitro Antifungal Activity of the Strain

The ability of the actinobacterial strain KRO3 to inhibit the growth of the phytopathogenic *Fusarium oxysporum* f. sp. *pisi* race 2 isolate F69 [21] was examined using a direct confrontation. Two 5 mm hyphal disks from one-week-old fungal culture grown on PDA plates (Potato Dextrose Agar—Potato Dextrose: Difco, Fisher Scientific Italia, Segrate (MI), Italy; supplemented with 1.5% *w/v* of agar) were manufactured and placed

at a distance of approximately 2.5 cm from the center of the Petri dish containing steak bacterial pre-culture. The tested bacterium was then streaked in the center of the same dish. After seven days of incubation at 28 °C, fungi mycelial growth was measured. The bacterial antagonistic capacity was assessed by calculating the percentage of inhibition of mycelial growth compared to the control, according to the formula reported by Zdorovenko et al., 2021 [22]. Petri dishes used as controls contained only two mycelial disks of the fungal strains. The experience was repeated thrice.

2.4. Bacterial Growth and Extraction of Bioactive Compounds

Plates of ISP2 agar medium, inoculated by pure culture of KRO3 strain, were incubated seven days at 30 °C. Culture medium was cut into small pieces and macerated in ethyl acetate overnight at room temperature as described by Leulmi et al. (2019) [23]. The extraction was repeated twice, and the combined organic extracts (TOE_{KRO3}) were dried with Na₂SO₄ and then evaporated under reduced pressure.

2.5. Antifungal Activity of the Organic Extract, Chromatographic Fractions (FA-FE), and Metacycloprodigiosin

Antifungal activities of TOE_{KRO3}, chromatographic fractions (FA-FE), and pure metacycloprodigiosin were tested against the phytopathogenic fungus *Fop*. The Minimal Inhibitory Concentration (MIC) of TOE_{KRO3} was evaluated as previously reported [24]. Briefly, a weighted amount of TOE_{KRO3} was dissolved in MeOH. This solution was serially diluted to obtain solutions at different concentrations of TOE_{KRO3}. Each solution (10 µL) was deposited on the center of a PDA plate. A 5 mm fungal disc of *Fop* taken from a one-week-old plate and deposited on the center of the Petri dish amended with the TOE_{KRO3} at concentrations ranging from 62.5 to 1000 µg/plug. Before depositing the fungus disc, the solvent was allowed to evaporate in a laminar flow cabinet, and the plates were incubated at 25 °C for 7 days. MeOH was used as a negative control. Fungal growth was evaluated on each plate and MIC was reported by calculating of growth percentage inhibition as previously reported [22], using the following formula:

$$\text{Growth inhibition (\%)} = \frac{(R_c - R_i)}{R_c} \cdot 100$$

where R_c is the radial growth of the test pathogen in the control plates (mm), and R_i is the radial growth of the test pathogen in the test plates (mm). The experiment was performed in triplicate.

The same protocol was used also to test the antifungal activities of the chromatographic fractions (FA-FE) at a concentration of 250 µg/plug and to determine the MIC of pure metacycloprodigiosin at concentrations ranging from 15.625 to 200 µg/plug.

2.6. Isolation of Bacterial Metabolites

A total of 100 mg of the bacterial organic extract was purified by column chromatography (CC) using as eluent CHCl₃/*i*-PrOH (95:5, *v/v*), yielding five groups (FA-FE) of homogeneous fractions of 18.7 (FA), 35.6 (FB), 7.4 (FC), 28.3 (FD), and 6.5 (FE) mg, respectively. The residue of FA, showing antifungal activity against *Fop*, was further purified by two steps on TLC eluted with CHCl₃/*i*-PrOH (98:2, *v/v*) and petroleum-ether/acetone (8:2) yielding a pure amorphous solid identified as metacycloprodigiosin (**1**, 8.6 mg).

Metacycloprodigiosin (1): red amorphous solid; $[\alpha]_D^{25}$ -2360 (*c* 0.1, CHCl₃) (ref. [25] $[\alpha]_D^{20}$ -2370); ESI-MS (+): *m/z* 392 [M + H]⁺; ¹H NMR (400 MHz, CDCl₃) 12.78 (bs, 1H, NH), 12.65 (bs, 1H, NH), 12.59 (bs, 1H, NH), 7.23 (m, 1H, H-1), 7.06 (s, 1H, H-9), 6.92 (m, 1H, H-3), 6.35 (m, 1H, H-2), 6.27 (d, 1H, *J* = 1.6 Hz, H-12), 6.10 (s, 1H, H-6), 4.03 (s, 3H, Me-25), 3.22 (m, 1H, H-14A), 2.76 (m, 1H, H-14B), 2.54 (m, 1H, H-22), 1.82–0.24 (m, 16H, H₂-15-21 and H₂-23), 0.89 (t, 3H, *J* = 6.2 Hz, Me-24); ¹³C NMR (100 MHz, CDCl₃) 165.5 (C-7), 154.5 (C-13), 150.4 (C-11), 147.4 (C-5), 126.8 (C-1), 126.0 (C-10), 122.3 (C-4), 120.6 (C-8),

116.8 (C-3), 113.3 (C-9), 112.4 (C-12), 111.6 (C-2), 92.7 (C-6), 58.7 (C-25), 39.6 (C-22), 29.9 (C-23), 29.1 (C-14), 34.4, 27.3, 26.8, 26.6, 25.6, 24.5, 22.7 (C-15-21), 12.6 (C-24).

2.7. GC-MS Analysis of Fractions FB-FE

GC-MS data were acquired on chromatographic fractions (FB-FE) after trimethylsilylation with *N,O*-bis(trimethylsilyl)trifluoroacetamide (BSTFA) (Fluka, Buchs, Switzerland) as previously reported [26]. GC-MS measurements were performed with an Agilent 6850 GC (Milan, Italy), equipped with an HP-5MS capillary column (5% phenyl methyl poly siloxane stationary phase), coupled to an Agilent 5973 Inert MS detector operated in the full scan mode (m/z 29–550) at a frequency of 3.9 Hz and with the EI ion source and quadrupole mass filter temperatures kept, respectively, at 200 °C and 250 °C. Helium was used as carrier gas at a flow rate of 1 mL/min. The injector temperature was 250 °C and the temperature ramp raised the column temperature from 70 °C to 280 °C: 70 °C for 1 min; 10 °C/min until reaching 170 °C; and 30 °C/min until reaching 280 °C. Then, it was held at 280 °C for 5 min. The solvent delay was 4 min. Compounds were identified by comparing their EI mass spectra at 70 eV with spectra present in the NIST 20 mass spectral library using NIST MS Search 2.4 (NIST 20, <https://www.nist.gov/srd/nist-standard-reference-database-1a> accessed on 20 October 2024). In addition, the identification was supported by the Kovats retention index (RI) calculated for each analyte by the Kovats equation, using the standard *n*-alkane mixture in the range C7-C40 (Sigma-Aldrich, Saint Louis, MO, USA).

2.8. Statistical Analysis

All the statistical analyses were performed using Minitab[®] 20.4 software. Data were expressed as mean \pm SEM. Differences among groups were compared by One-way ANOVA followed by a multiple comparison test whenever the ANOVA test was statistically significant at $p < 0.05$.

3. Results

3.1. The Strain KRO3

The physiological characteristics of strain KRO3 are summarized in Table 1. This filamentous, Gram-positive bacterium exhibits notable metabolic versatility, efficiently utilizing a broad spectrum of carbon sources for both growth and energy production. In addition, it can metabolize a variety of amino acids as nitrogen sources. Strain KRO3 has demonstrated tolerance to NaCl concentrations of up to 6% and possesses the ability to degrade gelatin and casein. The partial 16S rDNA gene sequence analysis demonstrated that the strain KRO3 was most likely *S. alboblavus* (Accession No. PQ328212).

Table 1. Physiological characteristics of bacterial isolate KRO3 ^a.

| Carbon Source Utilization | Nitrogen Source Utilization | Growth in the Presence of. . . | Degradation Activity |
|---------------------------|-----------------------------|--------------------------------|----------------------|
| Arabinose + | Histidine + | pH 4 – | Gelatin + |
| Fructose + | Arginine + | pH 7 + | Casein + |
| Galactose + | Tyrosine + | pH 9 + | Starch – |
| Inositol + | Alanine + | NaCl 6% <i>w/v</i> + | Cellulose – |
| Mannitol + | Glycine + | NaCl 8% <i>w/v</i> + | |
| Glucose + | Methionine + | NaCl 8% <i>w/v</i> + | |
| Lactose + | Valine + | Phenol 0.1% <i>w/v</i> + | |
| Rhamnose – | Leucine + | Penicillin 10 UI + | |
| Maltose + | Tryptophan + | Growth at 45 °C + | |
| Sucrose + | Asparagine + | Nitrate reduction + | |
| Sorbitol + | Proline + | | |
| Xylitol + | | | |
| Mannose + | | | |
| Xylose – | | | |

^a Plus sign (+) indicates a positive reaction; minus sign (–) indicates a negative reaction.

3.2. In Vitro Antifungal Activity of the Strain

The ability of *Streptomyces alboflavus* KRO3 to inhibit the growth of *Fop* was assessed through one-week direct confrontation test on PDA (Potato Dextrose Agar). Results revealed a significant inhibition rate of 91.00 ± 1.73 compared to the untreated control (Figure 1).

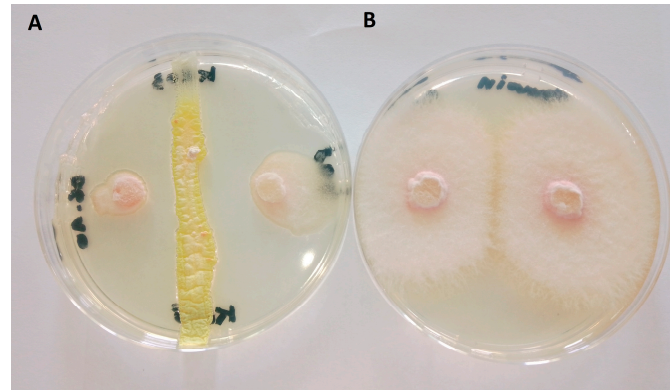


Figure 1. In vitro antifungal assay of the strain. (A) Growth inhibition of *F. oxysporum* f. sp. *pisi* by *Streptomyces alboflavus* KRO3; (B) *F. oxysporum* f. sp. *pisi* on Potato Dextrose Agar (PDA) as control.

3.3. Antifungal Activity of the Organic Extract

The bacterium isolate was cultured on ISP2 agar plates and extracted with EtOAc. The resulting organic extract (TOE_{KRO3}) was analyzed for its antifungal activity against *Fop* at concentrations ranging from 100 $\mu\text{g}/\mu\text{L}$ (1 mg/plug) to 6.25 $\mu\text{g}/\mu\text{L}$ (62.5 $\mu\text{g}/\text{plug}$) with MeOH serving as the negative control (Figure 2). As reported in Figure 2, the *S. alboflavus* KRO3 extract exhibited strong antifungal activity, maintaining an inhibition rate of approximately 90% at concentrations up to 250 $\mu\text{g}/\text{plug}$ compared to the control, indicating that the bacterial metabolites are effective against the fungus.

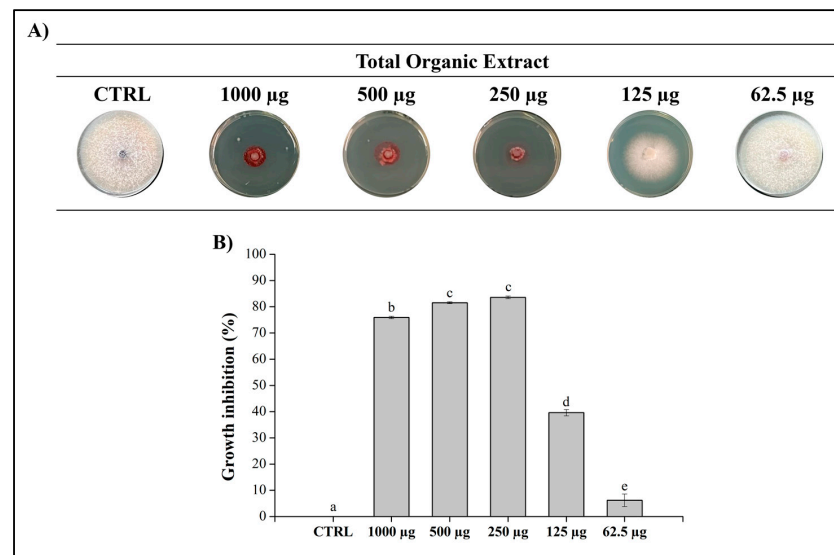


Figure 2. Antifungal assay of the organic extract. (A) The TOE_{KRO3} of *Streptomyces alboflavus* KRO3 was tested at 1000, 500, 250, 125, and 62.5 $\mu\text{g}/\text{plug}$ against *Fop* grown on PDA plates for 7 days at 25 $^{\circ}\text{C}$. MeOH was used as negative control; (B) graphical representation of the inhibition of the fungal growth of *Fop* by TOE_{KRO3}. Data are presented as means \pm S.E.M. ($n = 3$ replication for each concentration) compared to control *Fop* grown only with MeOH. One-way ANOVA test was performed to compare the groups of data; values that do not share a letter are statistically different ($p < 0.05$).

3.4. Fractionation of the Organic Extract and Evaluation of the Antifungal Activity

Given the notable antifungal activity of TOE_{KRO3} at a concentration of 250 µg/plug, the active extract was subjected to column chromatography to isolate and identify the specific compounds responsible for this potent activity. This fractionation process yielded five distinct fractions, labeled FA through FE. To assess their efficacy against *Fop*, each fraction was tested at the same concentration of 250 µg/plug. The results illustrated in Figure 3 highlight the differential antifungal activities exhibited by these fractions. The fractions FB, FC, FD, FE showed no antagonistic activity while FA was the only fraction exhibiting significant antifungal activity, achieving a 53% inhibition in fungal growth. This substantial inhibitory effect highlights FA as the primary fraction contributing to the antifungal potency of the original extract, TOE_{KRO3}.

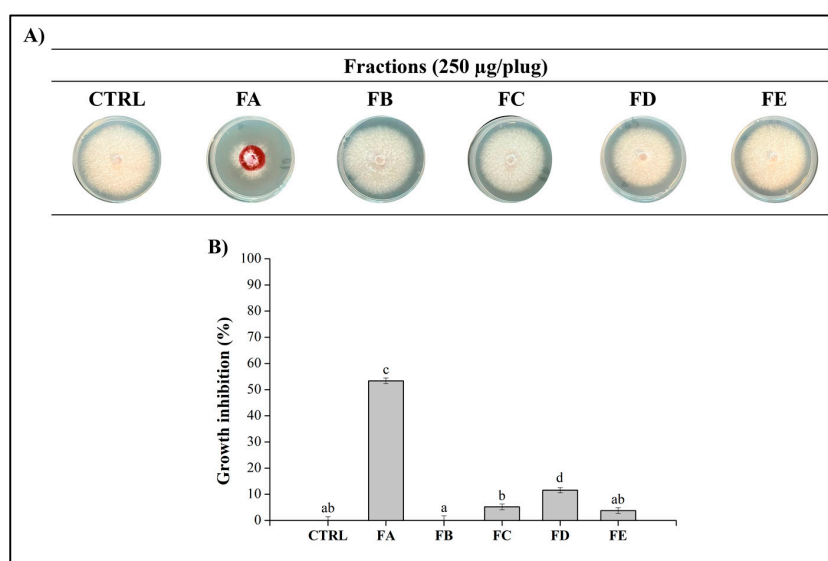


Figure 3. Antifungal assay of the fractions obtained from the organic extract. (A) The fractions of TOE_{KRO3} (from FA to FE) were tested at a concentration of 250 µg/plug against *Fop* grown on PDA plates for 7 days at 25 °C. MeOH was used as negative control. (B) Graphical representation of the inhibition of the fractions. Data are presented as means ± S.E.M. (n = 3 replication for each concentration) compared to control *Fop* grown only with MeOH. One-way ANOVA test was performed to compare the groups of data; values that do not share a letter are statistically different ($p < 0.05$).

3.5. Purification of Fraction FA

Fraction A was further purified by TLC yielding a pure compound which was identified as metacycloprodigiosin (**1**, Figure 4) comparing its spectroscopic (¹H and ¹³C NMR), spectrometric (ESI-MS), and physical (specific optical rotation) data with those reported in the literature [25,27].

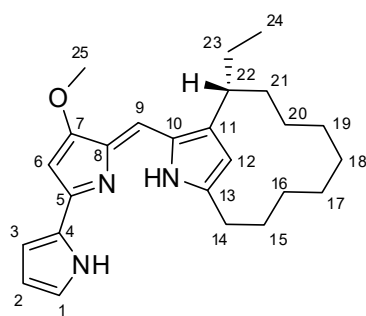


Figure 4. Chemical structure of metacycloprodigiosin (**1**).

In particular, its ^1H and ^{13}C NMR spectra (Figures S1 and S2) showed the typical signals patterns of the tripyrrole pigments belonging to the prodiginine family of bacterial alkaloids [28]. Furthermore, the same spectra are in agreement with the data previously reported by Kimata et al. (2017) [27] for metacycloprodigiosin (1). Its identification was confirmed using the data obtained from the ESI-MS spectrum recorded in the positive mode (Figure S3) that showed the protonated pseudomolecular ion $[\text{M}+\text{H}]^+$ peak at m/z 392. Finally, its configuration was confirmed by comparing the specific optical rotation value with that reported in the literature [25].

3.6. Antifungal Activity of Metacycloprodigiosin

To further confirm the responsibility of metacycloprodigiosin for the antifungal activity, we tested the pure compound on *Fop* at different concentrations to determine the MIC. By systematically varying the concentration of metacycloprodigiosin, we aimed to pinpoint the lowest concentration at which this compound effectively inhibits the growth of the fungus. Results reported in Figure 5 demonstrated a clear dose-dependent response, indicating that as the concentration of metacycloprodigiosin increased, the inhibition of fungal growth also increased correspondingly. At lower concentrations (from 62.5 $\mu\text{g}/\text{plug}$ down), the antifungal activity was moderate (less than 30% of *Fop* growth inhibition), but as the concentration approached the MIC (125 $\mu\text{g}/\text{plug}$), a significant reduction in fungal growth was observed. This sharp decline in growth near the MIC confirms the potent antifungal nature of metacycloprodigiosin. As reported in Figure 5, purified metacycloprodigiosin exhibited a significantly stronger antifungal effect than fraction FA, from which it was obtained, with an inhibition percentage of about 80% compared to 53% inhibition observed in fraction FA.

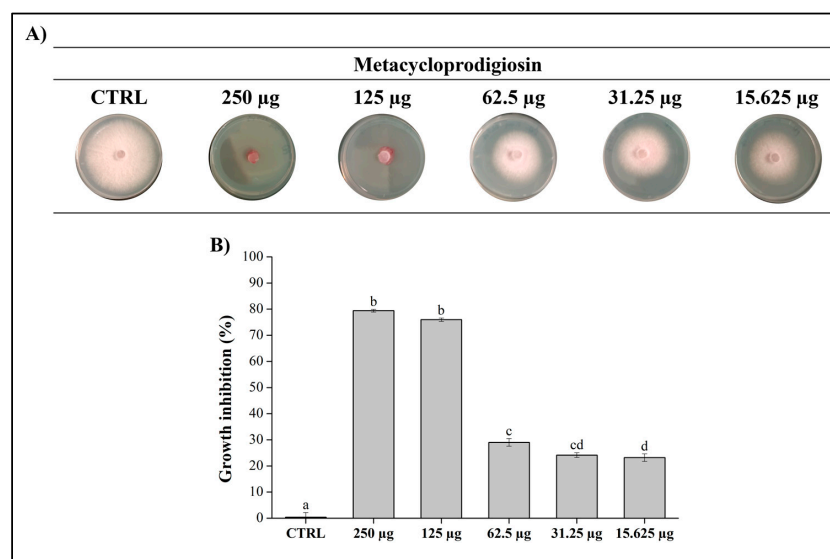


Figure 5. Antifungal assay of metacycloprodigiosin (1). (A) The metacycloprodigiosin was tested at 250, 125, 62.5, 31.25, and 15.625 $\mu\text{g}/\text{plug}$ against *Fop* grown on PDA plates for 7 days at 25 $^{\circ}\text{C}$. MeOH was used as negative control; (B) graphical representation of the inhibition of metacycloprodigiosin. Data are presented as means \pm S.E.M. ($n = 3$ replication for each concentration) compared to control *Fop* grown only with MeOH. One-way ANOVA test was performed to compare the groups of data; values that do not share a letter are statistically different ($p < 0.05$).

3.7. Identification of Metabolites in Fractions FB-FE

The four chromatographic fractions FB-FE were analyzed via GC-MS after trimethylsilylation (see Section 2), and the detected compounds are listed in Table 2. Several fatty acids and their esters were identified in fractions FB and FD, while 4-nitrobenzamide and furandimethanol were detected in fractions FC and FE, respectively (Figures S4 and S5). The identification of the latter compounds was further supported by NMR spectroscopy. In

fact, the ^1H NMR spectra of fractions FC and FE, recorded in CDCl_3 , showed the presence of 4-nitrobenzamide and furandimethanol signals, respectively (Figures S6 and S7) [29,30].

Table 2. Compounds identified in chromatographic fractions FB-FE obtained from organic extract of *S.alboflavus*. RI represents Kovats retention index and TMS is the trimethylsilyl function, $(\text{CH}_3)_3\text{Si}$.

| Compound | RT (min) | RI | Peak Area% |
|---|----------|------|------------|
| Fraction FB | | | |
| Myristic acid, TMS | 12.59 | 1814 | 6.88 |
| Pentadecanoic acid, TMS | 13.04 | 1915 | 45.46 |
| Palmitelaidic acid, TMS | 13.36 | 1994 | 2.65 |
| Palmitic acid, TMS | 13.42 | 2011 | 23.01 |
| Margaric acid, TMS | 13.81 | 2118 | 13.03 |
| 10-Heptadecenoic acid, TMS | 13.87 | 2137 | 8.69 |
| Oleic acid, TMS | 14.07 | 2192 | 0.28 |
| Fraction FC | | | |
| 4-Nitrobenzamide, TMS | 12.82 | 1864 | - |
| Fraction FD | | | |
| 1-Monomyrisitin, 2TMS | 14.72 | 2362 | 1.14 |
| 2-Monopalmitin, 2TMS | 14.98 | 2423 | 0.21 |
| Pentadecanoic acid, glycerine-(1)-monoester, 2TMS | 15.16 | 2461 | 25.88 |
| 1-Monopalmitin, 2TMS | 15.66 | 2559 | 36.28 |
| Heptadecanoic acid, glycerine-(1)-monoester, 2TMS | 16.25 | 2652 | 29.86 |
| 1-Monooleoylglycerol, 2TMS | 16.90 | 2746 | 6.64 |
| Fraction FE | | | |
| Furandimethanol (2TMS) | 9.54 | 1427 | - |

4. Discussion

The *Streptomyces alboflavus* KRO3 strain was characterized and found to exhibit very strong in vitro antifungal activity against *Fop* (Figure 1). The observed inhibition zone might suggest the presence of diffusible inhibitory substances in the medium that affected the growth of the pathogen (*Fop*). Previous studies described antagonistic activities of other strains of *Streptomyces* sp. against other formae speciales (ff.spp.) of *Fusarium oxysporum*, such as f. sp. *cubense* [13,31], f. sp. *lycopersici* [32,33], and f. sp. *ciceris* [34].

KRO3 was, thus, cultured in ISP2 agar medium to extract and characterize its bioactive secondary metabolites. The organic ethyl acetate extract of the sample showed an important antagonistic activity. However, the antifungal activity of the organic extract decreased slightly compared to that of the bacterium, suggesting that the bacterium's superior efficacy may result from various factors, such as the instability of certain bacterial compounds outside of the cellular environment, the loss of synergy due to selective extraction and solubility issues, the lack of physical interaction between molecules, or the absence of an induced response in the presence of fungi and the live bacteria. The ethyl acetate extract was subsequently fractionated using silica gel column chromatography to isolate and purify its bioactive compounds. Among the five fractions obtained from the organic extract, only the FA fraction showed significant antifungal activity, with a 53% inhibition in fungal growth, highlighting that FA is the main fraction contributing to the antifungal activity of the original extract, TOEK_{R03}. Purification of bioactive fraction FA by

chromatographic techniques led to the isolation of a pure compound which was identified as metacycloprodigiosin (1) [35].

GC-MS analysis of the further chromatographic fractions (FB-FE) led to the identification of fatty acids and monoglycerides in fractions FB and FD. Considering that fatty acids are ubiquitous molecules that are normally found bound to other compounds such as glycerol [36], it is not surprising to detect them in our samples. These findings can be further explained by the fact that fatty acids are essential components of the streptomycetes membrane with a role in bacterial survival and adaptation to different environmental conditions [37]. In the FC and FE fractions, 4-nitrobenzamide and furandimethanol were identified, confirming the ability of these bacteria to produce chemically diverse metabolites [38]. However, as said above, these four chromatographic fractions turned out to be very poorly active in inhibiting *Fop* (Figure 3).

Metacycloprodigiosin, isolated from fraction FA, is a derivative of prodigiosin which is an important natural red pigment, produced as a secondary metabolite by microorganisms [28]. Structurally, these compounds are distinguished by its unique structure consisting of three pyrrole rings and a pyrrolyl-dipyrrolyl-methene backbone, with a methoxy group at the C-4 position [39]. Other notable members of the prodiginine family include undecylprodigiosin, nonylprodigiosin, and roseophilin [28]. Prodiginine was originally isolated from the bacterium *Serratia marcescens*, but it can be secreted by many other bacteria, such as *Hahella chejuensis*, *Serratia nematodiphila*, *Streptomyces coelicolor*, *Serratia rubidaea*, and *Streptomyces griseovirides* [40]. Metacycloprodigiosin (1) was first isolated from *Streptomyces longisporus ruber* by Wasserman et al. (1966) [41], together to undecylprodigiosin but the structure was elucidated only some years later [35] and it was confirmed by total synthesis of a racemic samples [25]. Clift and Thompson (2009) [42] realized the enantioselective synthesis and the absolute configuration of the natural compound was shown to be (*R*) by comparison of its electronic circular dichroism spectrum with the synthetic one [43]. Recently, Peixoto et al. (2018) [44] suggested that (*R*)-metacycloprodigiosin can exist in three different tautomeric forms and the addition of HCl reduces this structural diversity to *syn*-(*R*)-metacycloprodigiosin-HCl and *anti*-(*R*)-metacycloprodigiosin-HCl each with hydrogens at C-9' and C-12 in *syn* or *anti* orientation [44].

The prodiginine group of compounds have become a new research area for scientists; it has attracted increasing interest due to its remarkable biological activities and diverse applications. This promising biomolecule is used in various sectors, including the food, cosmetic, textile, and pharmaceutical industries. Its properties include antimicrobial, immunosuppressive, antimalarial, antineoplastic, and anticancer effects [45,46]. Recent studies have rekindled interest in prodigiosin because of its reported profound biological activities [45]. The antifungal activity of our pure compound was evaluated against *Fop* at various concentrations to determine the MIC. The molecule showed a dose-dependent response with MIC (125 µg/plug) resulting in a significant reduction in fungal growth. This sharp decline in growth near the MIC confirms the potent antifungal nature of metacycloprodigiosin. In agricultural research, the class of prodiginines has been shown to exhibit significant activity against various plant pathogens. It was reported that prodigiosin can act against gray mold, through spore germination inhibition in *Botrytis cinerea* [47]. The purified red pigment of *Serratia marcescens* was found to be effective against plant parasitic nematodes *Radopholus similis* and *Meloidogyne javanica* [48]. Habash et al. (2020) [49] reported inhibition in the plant pathogenic fungi *Phoma lingam* and *Sclerotinia sclerotiorum*. Prodigiosin has also been observed to have a toxic effect on certain fungal species, such as *Batrachochytrium dendrobatidis*, *B. salamandriovorans*, *Pythium myriotylum*, *Rhizoctonia solani*, *Sclerotium rolfsii*, *Phytophthora infestans*, *Fusarium oxysporum*, and *Colletotrichum nymphaeae* [50].

This study investigates, for the first time, the antifungal effect of metacycloprodigiosin produced by *Streptomyces alboflavus*. The stark contrast in the efficacy between the pure metacycloprodigiosin and the FA fraction highlights the potential benefits of using the purified compound in antifungal applications. However, the difference between the 80% inhibition observed by TOE_{KRO3} and the 53% inhibition by FA alone suggests that the

higher efficacy of the total extract is likely due to synergistic interactions among its various molecules. Synergy among the compounds in TOE_{KRO3} likely plays a critical role in its enhanced antifungal activity. When the inhibition percentages of all individual fractions are combined, they only total approximately 90%, which matches the inhibition percentage of the total extract, suggesting additive effects of all fractions in inhibitory activity. This indicates that while FA is highly effective on its own, the presence of other fractions contributes additional antifungal effects, enhancing the overall potency of TOE_{KRO3} beyond the sum of its parts. Thus, further purification and characterization of high amount of the TOE_{KRO3} extract could lead to the discovery of additional active compounds produced with very low yield and a better understanding of the synergistic or antagonistic interactions within the extract. On the other hand, the findings establish a foundation for the future development of metacycloprodigiosin as a plant protection agent. To achieve this, it is essential to further optimize the culture conditions for metacycloprodigiosin production to obtain higher yields.

Supplementary Materials: The following supporting information can be downloaded at: <https://www.mdpi.com/article/10.3390/jof10110783/s1>, Figure S1. ¹H NMR spectrum of metacycloprodigiosin (1) (CHCl₃, 400 MHz). Figure S2. ¹³C NMR spectrum of metacycloprodigiosin (1) (CHCl₃, 100 MHz), Figure S3. ESI-MS spectrum of metacycloprodigiosin (1), recorded in positive mode. Figure S4. EI mass spectrum at 70 eV of 4-nitrobenzamide, TMS (RI = 1864). TMS = trimethylsilyl group. Figure S5. EI mass spectrum at 70 eV of furandimethanol, 2TMS (RI = 1427). TMS = trimethylsilyl group. Figure S6. ¹H NMR spectrum of FC (CHCl₃, 400 MHz). Figure S7. ¹H NMR spectrum of FE (CHCl₃, 400 MHz).

Author Contributions: Conceptualization, M.M., M.B. and A.C.; methodology, M.M., M.B., R.I. and A.C.; software, D.N., I.S., S.C. and M.M.S.; validation, M.M., M.B., A.A., R.I. and A.C.; formal analysis, M.M., D.N., I.S., M.M.S., K.K., S.C. and J.G.Z.; investigation, M.B.; resources, M.B., R.I. and A.C.; data curation, M.M., M.M.S., R.I. and M.B.; writing—original draft preparation, M.M., D.N., M.B., I.S., M.M.S. and I.S.; writing—review and editing, K.K., S.C., J.G.Z., A.A., R.I. and A.C.; supervision, M.B. and A.C.; project administration, M.B. and A.C.; funding acquisition, M.M., M.B., A.A., R.I. and A.C. All authors have read and agreed to the published version of the manuscript.

Funding: This research was carried out within the Program for the Finanziamento della Ricerca di Ateneo (FRA) 2022 dell'Università degli Studi di Napoli Federico II and within the Agritech National Research Center and received funding from the European Union Next-Generation EU (Piano Nazionale di Ripresa e Resilienza (PNRR)_Missione 4 Componente 2, Investimento 1.4_D.D. 1032 17/06/2022, CN00000022).

Institutional Review Board Statement: Not applicable.

Informed Consent Statement: Not applicable.

Data Availability Statement: Data is contained within the article or Supplementary Materials.

Acknowledgments: J.G.Z. thanks the University of Cadiz for the postdoctoral support with the Margarita Salas fellowship (2021-067/PN/MS-RECUAL/CD), funded by the NextGenerationEU programme of the European Union. D.N., M.B. and K.K. are grateful the Algerian Ministry of Higher Education and the PRFU project (D00L05ES250220220002)

Conflicts of Interest: The authors declare no conflicts of interest.

References

1. Rubiales, D.; Fondevilla, S.; Chen, W.; Gentzbittel, L.; Higgins, T.J.V.; Castillejo, M.A.; Singh, K.B.; Rispaill, N. Achievements and Challenges in Legume Breeding for Pest and Disease Resistance. *CRC Crit. Rev. Plant Sci.* **2015**, *34*, 195–236. [CrossRef]
2. Purohit, A.; Ghosh, S.; Chaudhuri, R.K.; Chakraborti, D. Biological Control of Fusarium Wilt in Legumes. In *Plant Stress Mitigators*; Elsevier: Amsterdam, The Netherlands, 2023; pp. 435–454.
3. Lal, D.; Dev, D.; Kumari, S.; Pandey, S.; Aparna; Sharma, N.; Nandni, S.; Jha, R.K.; Singh, A. Fusarium Wilt Pandemic: Current Understanding and Molecular Perspectives. *Funct. Integr. Genom.* **2024**, *24*, 41. [CrossRef]
4. Aslam, S.; Ghazanfar, M.U.; Munir, N.; Hamid, M.I. Managing Fusarium Wilt of Pea by Utilizing Different Application Methods of Fungicides. *Pak. J. Phytopathol.* **2019**, *31*, 81–88. [CrossRef]

5. Bani, M.; Rubiales, D.; Rispaill, N. A Detailed Evaluation Method to Identify Sources of Quantitative Resistance to *Fusarium Oxysporum* f. sp. *Pisi* Race 2 within a *Pisum* spp. Germplasm Collection. *Plant Pathol.* **2012**, *61*, 532–542. [[CrossRef](#)]
6. Navas-Cortés, J.A.; Hau, B.; Jiménez-Díaz, R.M. Effect of Sowing Date, Host Cultivar, and Race of *Fusarium Oxysporum* f. sp. *Ciceris* on Development of Fusarium Wilt of Chickpea. *Phytopathology* **1998**, *88*, 1338–1346. [[CrossRef](#)]
7. Momma, N.; Momma, M.; Kobara, Y. Biological Soil Disinfestation Using Ethanol: Effect on *Fusarium Oxysporum* f. sp. *Lycopersici* and Soil Microorganisms. *J. Gen. Plant Pathol.* **2010**, *76*, 336–344. [[CrossRef](#)]
8. Chen, Y.; Zhou, D.; Qi, D.; Gao, Z.; Xie, J.; Luo, Y. Growth Promotion and Disease Suppression Ability of a *Streptomyces* sp. CB-75 from Banana Rhizosphere Soil. *Front. Microbiol.* **2018**, *8*, 2704. [[CrossRef](#)]
9. Torres-Rodríguez, J.A.; Reyes-Pérez, J.J.; Quiñones-Aguilar, E.E.; Hernandez-Montiel, L.G. Actinomycete Potential as Biocontrol Agent of Phytopathogenic Fungi: Mechanisms, Source, and Applications. *Plants* **2022**, *11*, 3201. [[CrossRef](#)]
10. Jose, P.A.; Maharshi, A.; Jha, B. Actinobacteria in Natural Products Research: Progress and Prospects. *Microbiol. Res.* **2021**, *246*, 126708. [[CrossRef](#)]
11. Yun, T.Y.; Feng, R.J.; Zhou, D.B.; Pan, Y.Y.; Chen, Y.F.; Wang, F.; Yin, L.Y.; Zhang, Y.D.; Xie, J.H. Optimization of Fermentation Conditions through Response Surface Methodology for Enhanced Antibacterial Metabolite Production by *Streptomyces* sp. 1–14 from Cassava Rhizosphere. *PLoS ONE* **2018**, *13*, e0206497. [[CrossRef](#)]
12. Sharma, M.; Manhas, R.K. Purification and Characterization of Salvianolic Acid B from *Streptomyces* sp. M4 Possessing Antifungal Activity against Fungal Phytopathogens. *Microbiol. Res.* **2020**, *237*, 126478. [[CrossRef](#)] [[PubMed](#)]
13. Wei, Y.; Zhao, Y.; Zhou, D.; Qi, D.; Li, K.; Tang, W.; Chen, Y.; Jing, T.; Zang, X.; Xie, J.; et al. A Newly Isolated *Streptomyces* sp. YYS-7 with a Broad-Spectrum Antifungal Activity Improves the Banana Plant Resistance to *Fusarium Oxysporum* f. sp. *Cubense* Tropical Race 4. *Front. Microbiol.* **2020**, *11*, 1712. [[CrossRef](#)] [[PubMed](#)]
14. Aggarwal, N.; Thind, S.K.; Sharma, S. Role of Secondary Metabolites of Actinomycetes in Crop Protection. In *Plant Growth Promoting Actinobacteria*; Springer: Singapore, 2016; pp. 99–121.
15. Girão, M.; Ribeiro, I.; Ribeiro, T.; Azevedo, I.C.; Pereira, F.; Urbatzka, R.; Leão, P.N.; Carvalho, M.F. Actinobacteria Isolated From *Laminaria ochroleuca*: A Source of New Bioactive Compounds. *Front. Microbiol.* **2019**, *10*, 428916. [[CrossRef](#)]
16. Khenaka, K.; Loredana, C.; Benedetti, A.; Leulmi, N.; Boulahrouf, A. Effect of Capsicum annum cultivated in sub-alkaline soil on bacterial community and activities of cultivable plant growth promoting bacteria under field conditions. *Arch. Agron. Soil Sci.* **2019**, *65*, 1417–1430. [[CrossRef](#)]
17. Liu, D.; Coloe, S.; Baird, R.; Pedersen, J. Rapid Mini-Preparation of Fungal DNA for PCR. *J. Clin. Microbiol.* **2000**, *38*, 471. [[CrossRef](#)]
18. Castaldi, S.; Zorrilla, J.G.; Petrillo, C.; Russo, M.T.; Ambrosino, P.; Masi, M.; Cimmino, A.; Isticato, R. *Alternaria alternata* Isolated from Infected Pears (*Pyrus communis*) in Italy Produces Non-Host Toxins and Hydrolytic Enzymes as Infection Mechanisms and Exhibits Competitive Exclusion against *Botrytis cinerea* in Co-Infected Host Fruits. *J. Fungi* **2023**, *9*, 326. [[CrossRef](#)]
19. Lane, D. 16S/23S rRNA Sequencing. In *Nucleic Acid Techniques in Bacterial Systematics*; Stackebrandt, E., Goodfellow, M., Eds.; John Wiley and Sons: Chichester, UK, 1991; pp. 115–175.
20. Yoon, S.-H.; Ha, S.-M.; Kwon, S.; Lim, J.; Kim, Y.; Seo, H.; Chun, J. Introducing EzBioCloud: A Taxonomically United Database of 16S rRNA Gene Sequences and Whole-Genome Assemblies. *Int. J. Syst. Evol. Microbiol.* **2017**, *67*, 1613–1617. [[CrossRef](#)] [[PubMed](#)]
21. Bani, M.; Rispaill, N.; Evidente, A.; Rubiales, D.; Cimmino, A. Identification of the Main Toxins Isolated from *Fusarium oxysporum* f. sp. *Pisi* Race 2 and Their Relation with Isolates' Pathogenicity. *J. Agric. Food Chem.* **2014**, *62*, 2574–2580. [[CrossRef](#)] [[PubMed](#)]
22. Zdorovenko, E.L.; Dmitrenok, A.S.; Masi, M.; Castaldi, S.; Muzio, F.M.; Isticato, R.; Valverde, C.; Knirel, Y.A.; Evidente, A. Structural Studies on the O-Specific Polysaccharide of the Lipopolysaccharide from *Pseudomonas donghuensis* Strain SVBP6, with Antifungal Activity against the Phytopathogenic Fungus *Macrophomina phaseolina*. *Int. J. Biol. Macromol.* **2021**, *182*, 2019–2023. [[CrossRef](#)]
23. Leulmi, N.; Sighel, D.; Defant, A.; Khenaka, K.; Boulahrouf, A.; Mancini, I. Nigericin and Grisorixin Methyl Ester from the Algerian Soil-Living *Streptomyces youssoufiensis* SF10 Strain: A Computational Study on Their Epimeric Structures and Evaluation of Glioblastoma Stem Cells Growth Inhibition. *Nat. Prod. Res.* **2019**, *33*, 266–273. [[CrossRef](#)]
24. Masi, M.; Castaldi, S.; Sautua, F.; Pescitelli, G.; Carmona, M.A.; Evidente, A. Truncatenolide, a Bioactive Disubstituted Nonenolide Produced by *Colletotrichum truncatum*, the Causal Agent of Anthracnose of Soybean in Argentina: Fungal Antagonism and SAR Studies. *J. Agric. Food Chem.* **2022**, *70*, 9834–9844. [[CrossRef](#)] [[PubMed](#)]
25. Wasserman, H.H.; Keith, D.D.; Rodgers, G.C. The Structure of Metacycloprodigiosin. *Tetrahedron* **1976**, *32*, 1855–1861. [[CrossRef](#)]
26. Guida, M.; Salvatore, M.M.; Salvatore, F. A Strategy for GC/MS Quantification of Polar Compounds via Their Silylated Surrogates: Silylation and Quantification of Biological Amino Acids. *J. Anal. Bioanal. Tech.* **2015**, *6*, 1–16. [[CrossRef](#)]
27. Kimata, S.; Izawa, M.; Kawasaki, T.; Hayakawa, Y. Identification of a Prodigiosin Cyclization Gene in the Roseophilin Producer and Production of a New Cyclized Prodigiosin in a Heterologous Host. *J. Antibiot.* **2017**, *70*, 196–199. [[CrossRef](#)]
28. Hu, D.X.; Withall, D.M.; Challis, G.L.; Thomson, R.J. Structure, Chemical Synthesis, and Biosynthesis of Prodiginine Natural Products. *Chem. Rev.* **2016**, *116*, 7818–7853. [[CrossRef](#)] [[PubMed](#)]
29. Yang, H.; Li, Y.; Jiang, M.; Wang, J.; Fu, H. General Copper-Catalyzed Transformations of Functional Groups from Arylboronic Acids in Water. *Chem.–A Eur. J.* **2011**, *17*, 5652–5660. [[CrossRef](#)]
30. De, S.; Kumar, T.; Bohre, A.; Singh, L.R.; Saha, B. Furan-Based Acetylating Agent for the Chemical Modification of Proteins. *Bioorg. Med. Chem.* **2015**, *23*, 791–796. [[CrossRef](#)]

31. Qi, D.; Zou, L.; Zhou, D.; Zhang, M.; Wei, Y.; Zhang, L.; Xie, J.; Wang, W. Identification and Antifungal Mechanism of a Novel Actinobacterium *Streptomyces huiliensis* sp. Nov. Against *Fusarium oxysporum* f. sp. *Cubense* Tropical Race 4 of Banana. *Front. Microbiol.* **2021**, *12*, 722661. [[CrossRef](#)]
32. Abbasi, S.; Safaie, N.; Sadeghi, A.; Shamsbakhsh, M. *Streptomyces* Strains Induce Resistance to *Fusarium oxysporum* f. sp. *Lycopersici* Race 3 in Tomato Through Different Molecular Mechanisms. *Front. Microbiol.* **2019**, *10*, 1505. [[CrossRef](#)]
33. Pengproh, R.; Thanyasiriwat, T.; Sangdee, K.; Kawicha, P.; Sangdee, A. Antagonistic Ability and Genome Mining of Soil *Streptomyces* spp. against *Fusarium oxysporum* f. sp. *Lycopersici*. *Eur. J. Plant Pathol.* **2023**, *167*, 251–270. [[CrossRef](#)]
34. Amini, J.; Agapoor, Z.; Ashengroph, M. Evaluation of *Streptomyces* spp. against *Fusarium oxysporum* f. sp. *Ciceris* for the Management of Chickpea Wilt. *J. Plant Prot. Res.* **2016**, *56*, 257–264. [[CrossRef](#)]
35. Wasserman, H.H.; Rodgers, G.C.; Keith, D.D. Metacycloprodigiosin, a Tripyrrole Pigment from *Streptomyces longisporus* Ruber. *J. Am. Chem. Soc.* **1969**, *91*, 1263–1264. [[CrossRef](#)] [[PubMed](#)]
36. De Carvalho, C.; Caramujo, M. The Various Roles of Fatty Acids. *Molecules* **2018**, *23*, 2583. [[CrossRef](#)]
37. Ilic-Tomic, T.; Genčić, M.S.; Živković, M.Z.; Vasiljevic, B.; Djokic, L.; Nikodinovic-Runic, J.; Radulović, N.S. Structural Diversity and Possible Functional Roles of Free Fatty Acids of the Novel Soil Isolate *Streptomyces* sp. NP10. *Appl. Microbiol. Biotechnol.* **2015**, *99*, 4815–4833. [[CrossRef](#)] [[PubMed](#)]
38. Donald, L.; Pipite, A.; Subramani, R.; Owen, J.; Keyzers, R.A.; Taufa, T. *Streptomyces*: Still the Biggest Producer of New Natural Secondary Metabolites, a Current Perspective. *Microbiol. Res.* **2022**, *13*, 418–465. [[CrossRef](#)]
39. Kuo, Y.-Y.; Li, S.-Y. Solid-State Fermentation of Food Waste by *Serratia marcescens* NCHU05 for Prodigiosin Production. *J. Taiwan Inst. Chem. Eng.* **2024**, *160*, 105260. [[CrossRef](#)]
40. Paul, T.; Mondal, A.; Bandyopadhyay, T.K.; Mahata, N.; Bhunia, B. Downstream Process Development for Extraction of Prodigiosin: Statistical Optimization, Kinetics, and Biochemical Characterization. *Appl. Biochem. Biotechnol.* **2022**, *194*, 5403–5418. [[CrossRef](#)]
41. Wasserman, H.H.; Rodgers, G.C.; Keith, D.D. The Structure and Synthesis of Undecylprodigiosin. A Prodigiosin Analogue from *Streptomyces*. *Chem. Commun.* **1966**, *22*, 825–826. [[CrossRef](#)]
42. Clift, M.D.; Thomson, R.J. Development of a Merged Conjugate Addition/Oxidative Coupling Sequence. Application to the Enantioselective Total Synthesis of Metacycloprodigiosin and Prodigiosin R1. *J. Am. Chem. Soc.* **2009**, *131*, 14579–14583. [[CrossRef](#)]
43. Hu, D.X.; Clift, M.D.; Lazarski, K.E.; Thomson, R.J. Enantioselective Total Synthesis and Confirmation of the Absolute and Relative Stereochemistry of Streptorubin B. *J. Am. Chem. Soc.* **2011**, *133*, 1799–1804. [[CrossRef](#)]
44. Peixoto, D.; Ferreira, E.P.; Lourenço, A.M.; Johnson, J.L.; Lobo, A.M.; Polavarapu, P.L. (R)-Metacycloprodigiosin-HCl: Chiroptical Properties and Structure. *Chirality* **2018**, *30*, 932–942. [[CrossRef](#)] [[PubMed](#)]
45. Srilekha, V.; Krishna, G.; Sreelatha, B.; Jagadeesh Kumar, E.; Rajeshwari, K.V.N. Prodigiosin: A Fascinating and the Most Versatile Bioactive Pigment with Diverse Applications. *Syst. Microbiol. Biomanufacturing* **2024**, *4*, 66–76. [[CrossRef](#)]
46. Islan, G.A.; Rodenak-Kladniew, B.; Noacco, N.; Duran, N.; Castro, G.R. Prodigiosin: A Promising Biomolecule with Many Potential Biomedical Applications. *Bioengineered* **2022**, *13*, 14227–14258. [[CrossRef](#)]
47. Someya, N.; Nakajima, M.; Hirayae, K.; Hibi, T.; Akutsu, K. Synergistic Antifungal Activity of Chitinolytic Enzymes and Prodigiosin Produced by Biocontrol Bacterium, *Serratia marcescens* Strain B2 against Gray Mold Pathogen, *Botrytis cinerea*. *J. Gen. Plant Pathol.* **2001**, *67*, 312–317. [[CrossRef](#)]
48. Rahul, S.; Chandrashekhar, P.; Hemant, B.; Chandrakant, N.; Laxmikant, S.; Satish, P. Nematicidal Activity of Microbial Pigment from *Serratia Marcescens*. *Nat. Prod. Res.* **2014**, *28*, 1399–1404. [[CrossRef](#)] [[PubMed](#)]
49. Habash, S.S.; Brass, H.U.C.; Klein, A.S.; Klebl, D.P.; Weber, T.M.; Classen, T.; Pietruszka, J.; Grundler, F.M.W.; Schleker, A.S.S. Novel Prodigiosin Derivatives Demonstrate Bioactivities on Plants, Nematodes, and Fungi. *Front. Plant Sci.* **2020**, *11*, 579807. [[CrossRef](#)]
50. Araújo, R.G.; Zavala, N.R.; Castillo-Zacarias, C.; Barocio, M.E.; Hidalgo-Vázquez, E.; Parra-Arroyo, L.; Rodríguez-Hernández, J.A.; Martínez-Prado, M.A.; Sosa-Hernández, J.E.; Martínez-Ruiz, M.; et al. Recent Advances in Prodigiosin as a Bioactive Compound in Nanocomposite Applications. *Molecules* **2022**, *27*, 4982. [[CrossRef](#)]

Disclaimer/Publisher’s Note: The statements, opinions and data contained in all publications are solely those of the individual author(s) and contributor(s) and not of MDPI and/or the editor(s). MDPI and/or the editor(s) disclaim responsibility for any injury to people or property resulting from any ideas, methods, instructions or products referred to in the content.